Tabersonine affects osteoclast differentiation, apoptosis and ameliorates bone loss in osteoporotic mice

Hui Shi,[1,2,3]* Pinghui Zhou,[1]* Jingxian Fan,[2,3,4] Zhihui Wang,[2,3] Chengfeng Xu,[3,5] Nan Zhang,[3] Shiying Bian,[3] Xu Weng,[3] Qin Yang,[3] Mengying Xu,[6] Xishuai Tong,[7] Yingxiao Fu[1,2,3]

[1]Anhui Province Key Laboratory of Tissue Transplantation, Bengbu Medical University, Bengbu, Anhui
[2]Anhui Province Key Laboratory of Translational Cancer Research, Bengbu Medical University, Bengbu, Anhui
[3]Life Science School, Bengbu Medical University, Bengbu, Anhui
[4]Public Fundamentals School, Bengbu Medical University, Bengbu, Anhui
[5]Wuxi Blood Center, Wuxi,
[6]Clinical Medical School, Bengbu Medical University, Bengbu, Anhui
[7]Joint International Research Laboratory of Agriculture and Agri-Product Safety of the Ministry of Education of China, Institute of Agricultural Science and Technology Development, College of Veterinary Medicine, Yangzhou University, Yangzhou, Jiangsu, China

*These authors contributed equally to this work.

ABSTRACT

This study investigates the effects of tabersonine on osteoclast differentiation, apoptosis, and bone loss in osteoporotic mice. To address these objectives, we performed a series of in vitro and in vivo experiments. In vitro, RAW264.7 cell viability was assessed using the CCK-8 method, and osteoclast-like cells were induced with RANKL. The impact of tabersonine on osteoclast-like cell differentiation was assessed via TRAP staining, while DAPI and TRITC-Phalloidin staining were used to examine nuclear morphology and actin filament organization. Apoptosis in mature osteoclast-like cells was evaluated using Hoechst 33258 staining, and intracellular ROS levels were measured using a commercial assay kit. The expression of genes associated with osteoclast differentiation and apoptosis was analyzed by quantitative real-time PCR, and corresponding protein levels were determined *via* Western blotting. *In vivo*, an osteoporosis mouse model was established and treated with tabersonine. The femurs were collected and subjected to micro-CT reconstruction, H&E staining, and TRAP staining to evaluate the extent of bone loss. The results demonstrated that *in vitro*, tabersonine significantly inhibited osteoclast-like cell differentiation, accompanied by reduced expression of key differentiation-related genes, including MMP-9 and NFATc1, and altered activation of differentiation-associated proteins such as NFATc1, C-Fos, and C-Jun. Furthermore, tabersonine promoted apoptosis in mature osteoclast-like cells, as evidenced by upregulated apoptosis-related genes (Caspase-3 and Bax) and proteins (Caspase-3, Bax, Bcl-2, and Caspase-9). *In vivo*, tabersonine ameliorated bone loss parameters and reduced osteoclast numbers in femoral tissues of osteoporotic mice. Collectively, these findings suggest that tabersonine suppresses osteoclast-like cell differentiation and facilitates apoptosis of mature osteoclast-like cells, thereby effectively attenuating bone loss in osteoporotic mice.

Key words: tabersonine; osteoclast; osteoporosis; bone loss.

Correspondence: Yingxiao Fu, Life Science School, Bengbu Medical University, Bengbu 233030, Anhui, China. E-mail: fuyingxiao8415@163.com

Contributions: Hui Shi, writing – original draft, visualization, validation, software, resources, methodology, investigation, formal analysis, data curation, conceptualization, writing – review & editing. Pinghui Zhou, visualization, validation, software, resources, methodology, investigation, formal analysis, funding acquisition. Jingxian Fan, visualization, validation, software, resources. Zhihui Wang, visualization, resources, methodology, investigation. Chengfeng Xu, visualization, validation, software. Nan Zhang, software, resources. Shiying Bian, resources, investigation. Xu Weng, validation, software. Qin Yang, resources, methodology. Mengying Xu, resources, investigation. Xishuai Tong, visualization, validation. Yingxiao Fu, writing – original draft, visualization, validation, software, resources, methodology, investigation, formal analysis, data curation, writing – review & editing, supervision, funding acquisition, conceptualization, project administration.

Conflict of interest: the authors declare that the research was conducted in the absence of any commercial or financial relationships that could be construed as a potential conflict of interest.

Ethics approval: all animal experiments were conducted in accordance with the approval of the Animal Experimentation Ethics Committee at Bengbu Medical University (Approval No. 2025668).

Funding: this work was supported by the Project of Natural Science Foundation of Anhui Province (grant No. 1908085MH276), The Natural Science Research Project of Anhui Provincial Department of Education (grant No. 2024AH051199), the Project of Anhui Province Key Laboratory of Tissue Transplantation (AHTT2024A003) and Anhui Province college students innovation and entrepreneurship training program projects (S202410367143, S202310367027, S202210367054).

Data Availability Statement: the data used to support the findings of this study are available from the corresponding author on reasonable request.

Introduction

With the global population aging, osteoporosis has become a significant health concern garnering increasing attention.[1,2] At the cellular level, osteoporosis arises from an imbalance in bone remodeling, in which bone resorption exceeds bone formation. This imbalance results in decreased bone mass and compromised bone microstructure.[3] The dynamic equilibrium of bone remodeling is critical for maintaining skeletal bone mass and primarily involves osteoclast-mediated bone resorption alongside osteoblast-mediated bone formation.[4] Osteoclasts derive from the fusion of multiple monocytes, and their differentiation is predominantly regulated by signals such as receptor activator of nuclear factor kappa-B ligand (RANKL) and macrophage colony-stimulating factor (M-CSF).[5] RANKL binds to its receptor RANK on osteoclast precursor cells, thereby triggering a series of signaling cascades involving the nuclear factor kappa-B (NF-κB) family, the MAPK family, and the transcription factor nuclear factor of activated T cells c1 (NFATc1).[6] The transcription factor NFATc1 promotes osteoclast formation and activity by driving the expression of genes linked to osteoclast differentiation and activation, including matrix metallopeptidase 9 (MMP-9), cathepsin K (CTSK), and acid phosphatase (Acp5).[7] Moreover, osteoclasts undergo polarization during differentiation and maturation, with their ruffled membranes attaching to the mineralized surface of cortical or cancellous bone, thereby creating a relatively confined microenvironment that favors bone resorption. This process is further facilitated by the acidic environment generated during resorption. Ultimately, mature osteoclasts undergo apoptosis, which reduces bone resorption. Inhibiting bone resorption can help mitigate bone loss and support the maintenance of bone density.[8] Therefore, modulating osteoclast differentiation, activation, and apoptosis represents a promising therapeutic strategy for combating osteoporosis at the cellular level.[9]

Currently, the primary drugs used in the clinical management of osteoporosis include bone formation promoters, bone resorption inhibitors, and bone metabolism modifiers. However, each of these therapies carries specific adverse effects and limitations.[10] Consequently, there is a pressing need for further research and the development of novel pharmacological options. The pharmacodynamics and pathology of natural compounds have emerged as significant research areas across various disciplines and have shown promise in clinical practice. Tabersonine, a terpene indole alkaloid originally isolated from the periwinkle plant of the family Apocynaceae, is soluble in dimethyl sulfoxide (DMSO).[11] This compound exhibits a range of biological activities, including anti-inflammatory, anti-tumor, and neuroprotective effects.[12-14] In the context of osteoporosis prevention, existing studies have primarily focused on its impact on osteoblast activity.[15] Notably, there is a paucity of literature addressing the effects of tabersonine on osteoclast formation, activity, and survival. This paper aims to elucidate the molecular mechanisms by which tabersonine regulates osteoclast differentiation, activation, and apoptosis, thereby potentially offering a theoretical framework for the prevention and treatment of osteoporosis associated with abnormal osteoclast activity.

Materials and Methods

The RAW264.7 cell line was obtained from the Cell Bank of the Committee on Preservation of Typical Cultures at the Chinese Academy of Sciences (Shanghai, China). Female C57/BL6 mice, aged 4 to 6 weeks, were acquired from Hangzhou Ziyuan Laboratory Animal Technology Co., Ltd. All animal experiments were conducted in accordance with the approval of the Animal Experimentation Ethics Committee at Bengbu Medical University (Approval No. 2025668). Tabersonine was procured from MedChemExpress (MCE, Shanghai, China). RANKL was sourced from PeproTech (Cranbury, NJ, USA). The tartrate-resistant acid phosphatase (TRAP) kit was obtained from Merck (Rahway, NJ, USA). The reverse transcription kit (PrimeScript™ RT Reagent Kit with Perfect Real Time) and the quantitative PCR kit (TB Green® Premix Ex Taq™ with Tli RNaseH Plus) were purchased from Takara Corporation (Shiga, Japan). Antibodies against C-Fos, C-Jun, NFATC1, Bcl-2, Caspase-3, Bax, and Caspase-9 were acquired from Cell Signaling Technology (Danvers, MA, USA).

Effect of tabersonine on RAW264.7 cell viability as determined by CCK-8 assay

RAW264.7 cells were seeded in 96-well plates at a density of 3,000 cells per well and cultured overnight. Subsequently, different concentrations of tabersonine (0, 0.625 μM, 1.25 μM, 2.5 μM, 5 μM, 10 μM, and 15 μM) were added to each group. After 36 h of incubation, Cell Counting Kit-8 (CCK-8) solution (5 mg/mL) was added to each well and incubated in the dark for 3 h. The absorbance was measured at 570 nm using a multifunctional microplate reader (Bio-Tek Instruments, Winooski, VT, USA).

Effect of tabersonine on osteoclast-like cell differentiation by TRAP staining

RAW264.7 cells were seeded into 96-well plates at a density of 5,000 cells per well. After cell attachment, RANKL was added at a concentration of 100 ng/mL. Over a period of 5-7 days of induction culture, various concentrations of tabersonine (0, 0.625 μM, 1.25 μM, 2.5 μM, 5 μM, and 10 μM) were added to each group. After 36 h, cells were subjected to TRAP staining. Briefly, prior to staining, deionized water was preheated, and the cells in each well were fixed by the addition of 100 μL of 4% paraformaldehyde for 10 min. Staining was performed using a solution prepared from Sodium Nitrite and Fast Garnet GBC base, which was allowed to stand for 5 min in the dark before being diluted with deionized water. Next, Naphthol AS-BI Phosphate Solution, Acetate Solution, and Tartrate Solution were sequentially added to the mixture, followed by thorough mixing of the staining solution. An aliquot of 200 μL of this staining solution was then added to each well and incubated at 37°C for 1 h. To prevent drying, 50 μL of deionized water was added to each well after incubation. Finally, stained cells were examined and photographed using an inverted microscope (Olympus Co., Ltd., Tokyo, Japan).

The effect of tabersonine on the morphology of osteoclast-like cells as determined by DAPI and TRITC phalloidin staining

RAW264.7 cells were seeded into 96-well plates at a density of 5,000 cells/well, and after attachment, RANKL was added at a concentration of 100 ng/mL. During a 5–7 day induction culture, varying concentrations of tabersonine (0, 0.625 μM, 1.25 μM, 2.5 μM, 5 μM, and 10 μM) were added to the respective groups. After 36 h, cells were subjected to 4’,6-diamidino-2-phenylindole dihydrochloride (DAPI) and TRITC-Phalloidin staining. Briefly, cells in each well were fixed with 100 μL of 4% paraformaldehyde for 15 min, followed by permeabilization with 100 μL of Triton X-100 solution for 5 min. Subsequently, TRITC-phalloidin staining solution (1:100 dilution in PBS) was added to the wells and incubated for 20 min in the dark. Afterward, DAPI staining solution at a

OPEN ACCESS

working concentration of 6 μg/mL was added and incubated for an additional 15 min. Finally, an anti-fluorescence quenching mounting medium was applied to the plates, which were then examined using a fluorescence microscope to observe the morphology of osteoclast-like cell nuclei and actin rings, with photographs taken for documentation (inverted fluorescence microscope; MF53-N, Guangzhou Micro-shot Technology Co., Ltd., Guangzhou, China).

Morphologic effects of tabersonine on apoptosis of mature osteoclast-like cells as determined by Hoechst 33258 staining

RAW264.7 cells were seeded into 96-well plates at a density of 5,000 cells/well, and RANKL was added at a concentration of 50 ng/mL after cell attachment. Various concentrations of tabersonine (0, 0.625 μM, 1.25 μM, 2.5 μM, 5 μM, and 10 μM) were added during a 3 d induction culture. After 36 h, cells were subjected to Hoechst 33258 staining. Briefly, the cells were washed three times with PBS, and 50 μL of Hoechst 33258 staining solution was added to each well. The samples were incubated at 37°C for 30 min in the dark, followed by immediate observation and photography using a fluorescence microscope.

ROS detection kit to analyze the effect of tabersonine on ROS production in osteoclast-like cells

RAW264.7 cells were seeded in 6-well plates at a density of 4 × 10^5 cells per well. After cell attachment, RANKL (50 ng/mL) was added. Various concentrations of tabersonine (0, 0.625 μM, 1.25 μM, 2.5 μM, 5 μM, and 10 μM) were added to each group during a 3 d induction culture period. After 36 h, the cells were harvested and washed with PBS. The DCFH-DA probe was then diluted in serum-free culture medium at a ratio of 1:1000 to achieve a final concentration of 10 μM DCFH-DA, which was added to the cells and incubated at 37 °C in a light-protected environment for 20 min. At the conclusion of the incubation, the cells were washed three times with serum-free medium, and the ROS fluorescence intensity was assessed using either a fluorescence microscope or flow cytometry (CytoFLEX S; Beckman Coulter, Brea, CA, USA).

Effect of tabersonine on the level of key genes for osteoclast-like cell differentiation and apoptosis and apoptosis as determined by qRT-PCR assay

RAW264.7 cells were seeded in 6-well plates at a density of 4 × 10^5 cells per well. Following cell attachment, RANKL (100 ng/mL) was added. Different concentrations of tabersonine (0, 0.625 μM, 1.25 μM, 2.5 μM, 5 μM, and 10 μM) were added to each group during a 3-d induction culture. After 36 h, cells were harvested for total RNA extraction using the Trizol method, and the RNA was quantified and reverse transcribed into cDNA. PCR amplification was performed under the following conditions: initial pre-denaturation at 95°C for 30 s, followed by 40 cycles of 95°C for 5 s and 60°C for 34 s (Applied Biosystems, Waltham, MA, USA). The relevant primer sequences were as follows: NFATc1 (forward: GGGAAACGGAAGAGAAGCCA; reverse: ACCTCCTCTCAGCTCACTCT), MMP-9 (forward: GCCCTGGAACTCACACGACA; reverse: TTGGAAACTCACACACGCCAGAAG), Caspase-3 (forward: GGCTGACTTCCTGTATGCTTACTCTAC; reverse: ACTCGAATTCCGTTGCCACCTTC), Bax (forward: CGTGAGCGGCTGCTTGTCTG; reverse: TGGTGAGCGAGGCGGTGAG), and Bcl-2 (forward: TCCTTCCAGCCTGAGAGCAACC; reverse: TCACGACGGTAGCGACGAGAG).

Effect of tabersonine on changes in the levels of key proteins of osteoclast-like cell differentiation and apoptosis as determined by Western blotting assay

RAW264.7 cells were seeded into 6-well plates at a density of 4×10^5 cells per well. Following cell attachment, RANKL was added at a concentration of 50 ng/mL. Various concentrations of tabersonine (0, 0.625 μM, 1.25 μM, 2.5 μM, 5 μM, and 10 μM) were added to each group during a 3 d induction culture. After 36 h, cells were harvested for total protein extraction. Proteins were lysed on ice, centrifuged, and the supernatant was obtained and quantified using the BCA kit. After adding 5× loading buffer, protein samples were subjected to SDS-PAGE for separation, and then transferred onto a PVDF membrane. The membrane was blocked at room temperature for 2 h before being incubated overnight at 4°C with the primary antibody. After washing, the secondary antibody was applied and incubated at room temperature for 1 h. The membrane was subsequently washed again and incubated at room temperature for an additional hour. Finally, the membrane was placed in a chemiluminescent imaging system for exposure after the application of the developer solution.

Establishment of osteoporosis model mice with femoral tissue collection

Ovariectomized (OVX) mice are frequently employed as a model for studying postmenopausal osteoporosis due to their induced hormonal deficiency.[16] Consequently, this study extended beyond in vitro experiments to include animal studies investigating the effect of Tabersonine on bone loss in osteoporotic mice. C57/BL6 mice were housed under a controlled environment of 22±2°C, with 60% humidity, and a 12 h light/dark cycle, with food and water provided ad libitum. After a 7 d acclimatization period, the mice were anesthetized with 1% pentobarbital. The dorsal fur was removed, and they were positioned prone before being sterilized with iodophor. A median incision was made on both sides of the spine to access the ovaries. In the surgical group (ovariectomy, OVX), both ovaries were removed, whereas in the sham-operated group (Sham), the incision was made without ovary removal. After the surgery, the incision was closed and sterilized with iodine povidone. The mice were monitored until they regained consciousness. The study groups were as follows: Sham group, OVX group, and OVX + tabersonine group (OVX + Tab). At 3 d post-surgery, 20 mg/kg of Tabersonine was administered intraperitoneally to the OVX + Tab group, whereas the same volume of DMSO (the solvent for Tabersonine) was given to the Sham and OVX groups. Mice were injected every 48 h for a total of 6 weeks. At the conclusion of the experiment, the mice were euthanized, and their bilateral femurs were isolated. Attached tendons and fascia were removed, and the femurs were fixed in a 4% paraformaldehyde solution for 2 d.

Effect of tabersonine on bone microstructure in osteoporosis model mice as determined by micro-CT

Following fixation, femoral tissue was examined using a Skyscan 1276 CT scanner (Bruker, Ettlingen, Germany) with scanning parameters set at 80 kV for voltage, 80 mA for current, and a resolution of 10 μm. Upon completion of the scanning, SkyScan NRecon software was utilized for 3D reconstruction of bone tissues in selected regions. Key parameters were collected and analyzed, including bone volume (BV), total volume (TV), bone volume/total volume (BV/TV), trabecular thickness (Tb.Th), trabecular number (Tb.N), trabecular separation (Tb.Sp), bone mineral density (BMD), and cortical width (Ct.Th).

Effect of tabersonine on osteoclast area percentage and trabecular area percentage of bone

Following fixation, femoral tissues were decalcified using a 10% tetracycline-EDTA solution for four weeks. The femurs were subsequently dehydrated through a series of ethanol concentration gradients (50%, 70%, 80%, 95%, and 100%). After clearing in xylene, the samples were embedded in paraffin, sectioned into 4 µm slices, and placed in an oven for 1-2 h for temporary preservation or histological staining. TRAP staining was performed according to the previously established methods used for *in vitro* cell staining experiments,[17] whereas hematoxylin and eosin (H&E) staining was also utilized. The tissue sections were stained, allowed to air dry, sealed with neutral resin, and then examined under a microscope and photographed. TRAP staining was employed to evaluate the effect of tabersonine on the ratio of osteoclast surface area to bone surface area (Oc.S/BS) in a murine model of osteoporosis. H&E staining was utilized to assess the effect of Tabersonine on the ratio of trabecular bone area (TBA) in the same model.

Statistical analyses

All data were replicated three times and subjected to analysis using GraphPad Prism version 8.0.1 software. Results are presented as mean ±SEM, and one-way ANOVA was applied among groups. A probability value of less than 0.05 was considered significant (*p*-value: ns = not statistically significant, **p*<0.05, ***p*<0.01, ****p*<0.001).

Results

Effect of tabersonine on the viability of RAW264.7 cells

CCK-8 assay results indicated that, with the exception of the 15 µM concentration group, the other concentrations (0.625 µM, 1.25 µM, 2.5 µM, 5 µM, and 10 µM) of tabersonine did not significantly affect the viability of RAW264.7 cells ($p>0.05$). This suggests that lower concentrations of tabersonine did not exhibit apparent cytotoxicity toward RAW264.7 cells (Figure 1), thereby informing the selection of concentrations for subsequent experimental treatments.

Effect of tabersonine on osteoclast-like cell differentiation

TRAP cytochemical staining revealed that RANKL-differentiated osteoclast-like cells within the vehicle control group present-

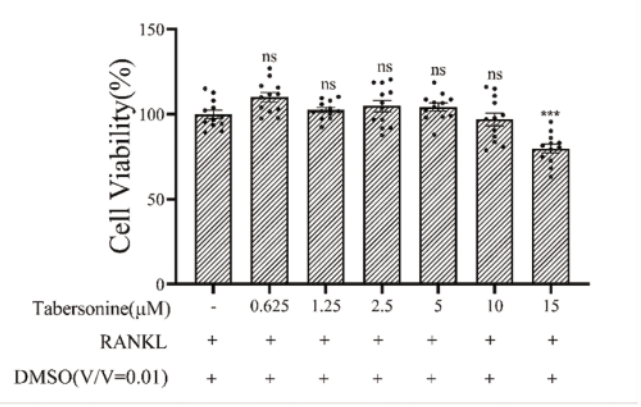


Figure 1. Effect of tabersonine on cell viability of RAW264.7. RAW264.7 was inoculated in 96 well plates and treated with different concentrations of tabersonine for 36 h. The cell viability was detected using CCK-8 kit. Results are expressed as the means ± SEM. Ns, not statistical significance, **p*<0.05, ***p*<0.01, ****p*<0.001 *vs* control.

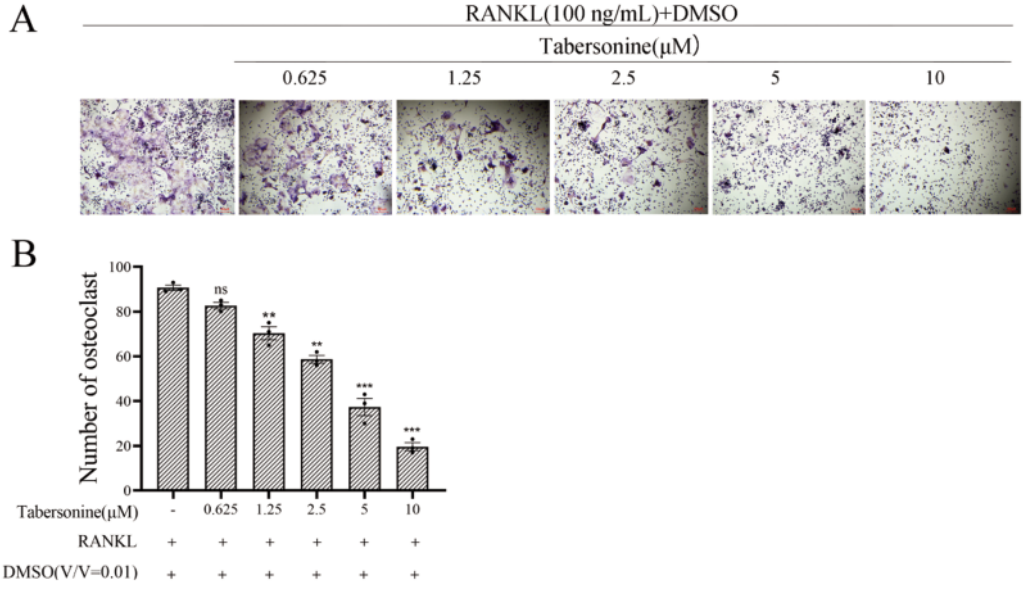


Figure 2. Tabersonine inhibits osteoclast-like cell differentiation formation. **A**) RANKL induced RAW264.7 was cultured for 5-7 d; different concentrations of tabersonine were added to each group, and TRAP staining was performed at the end of the culture, and the morphology of osteoclast-like cell in each group was shown in the graph (100×). **B**) Comparison of the number of osteoclast-like cell in each group. Results are expressed as the means ± SEM. Ns, not statistical significance, **p*<0.05, ***p*<0.01, ****p*<0.001 *vs* control.

OPEN ACCESS

ed enlarged cellular somata, abundant nuclei per cell, and characteristic purplish-red TRAP-positive cytoplasmic staining, indicative of robust multinucleated cell formation. In contrast, tabersonine intervention markedly attenuated osteoclast maturation, as evidenced by diminished cellular volume and fewer nuclei per cell, accompanied by suppressed multinucleation (Figure 2A). Specifically, the number of TRAP-positive osteoclast-like cells in the 1.25 μM (70.33±2.91), 2.5 μM (58.67±1.76), 5 μM (37.33±3.84), and 10 μM (19.67±1.76) tabersonine groups was markedly reduced relative to the control group (90.67±1.20). These differences reached statistical significance at $p<0.01$ or $p<0.001$, demonstrating a clear dose-dependent inhibitory effect (Figure 2B). Collectively, these results indicate that tabersonine potently suppresses RANKL-triggered osteoclastogenic differentiation of RAW264.7 cells.

Effect of tabersonine on the cytoskeleton and nucleus of osteoclast-like cells

DAPI and TRITC-conjugated phalloidin co-staining revealed that RANKL-induced osteoclast-like cells in the control group formed intact, well-spread F-actin rings with obvious multinucleation. Conversely, tabersonine exposure severely disrupted F-actin cytoskeletal assembly, with the most severe morphological impairment observed at 5 μM and 10 μM. At these concentrations, continuous intact F-actin rings were barely detectable, and most cells exhibited mononuclear features (Figure 3).

Effect of tabersonine on the expression of key genes for osteoclast-like Cell differentiation

Results from qRT-PCR experiments demonstrated that Tabersonine inhibited the mRNA expression of MMP-9 and NFATc1, which are genes associated with differentiation during the

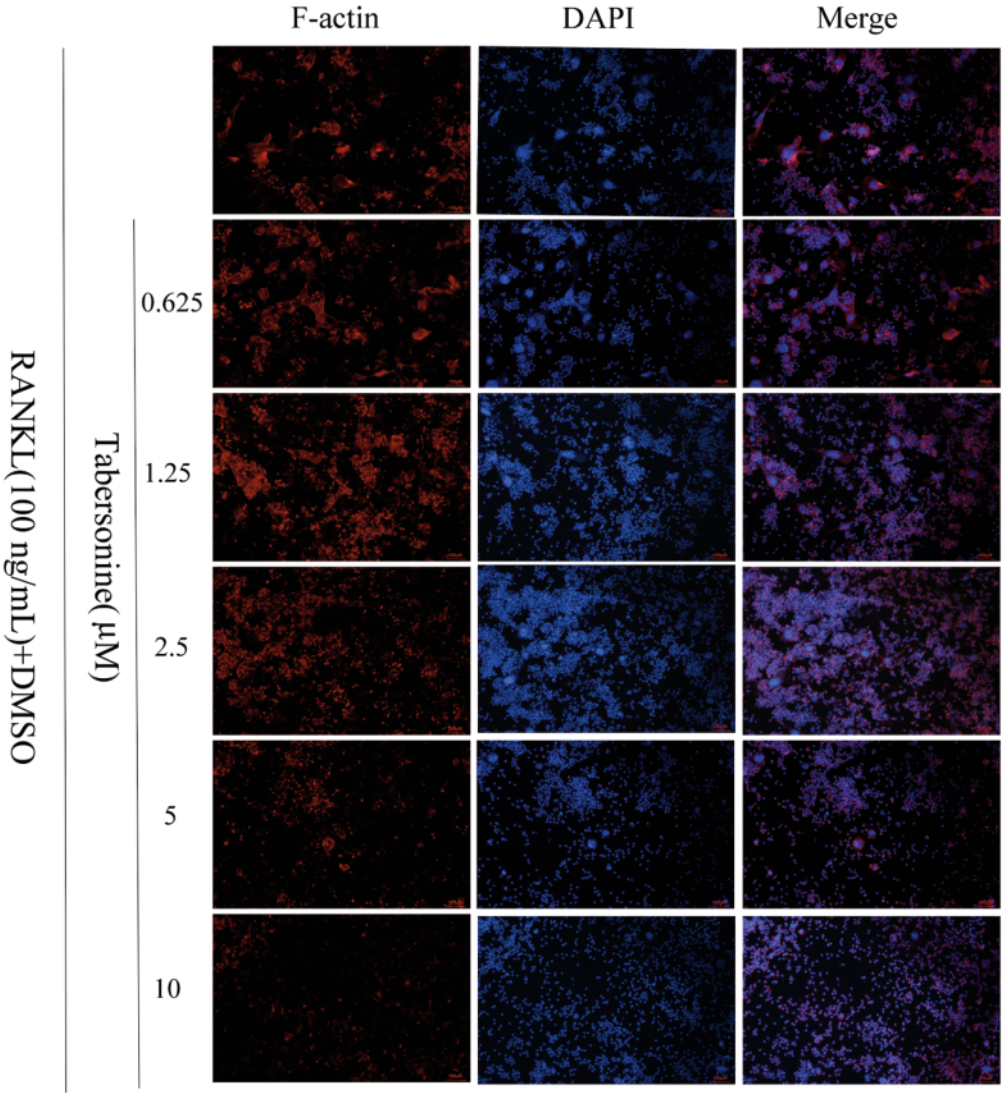


Figure 3. Tabersonine inhibits F-actin ring formation in osteoclast-like cells. RANKL induced RAW264.7 was cultured for 5-7 d. Different concentrations of Tabersonine were added to each group, and the culture was continued for 36 h. DAPI and TRITC Phalloidin staining was performed at the end of culture. The morphology of F-actin rings and nuclei within osteoclast-like cells in each group is shown (100×).

formation of osteoclast-like cells, in a dose-dependent manner compared with the control group (RANKL only). Notably, expression levels were significantly down-regulated in the 10 μM Tabersonine group (p<0.001) (Figure 4).

Effect of tabersonine on changes in the levels of proteins critical to osteoclast-like cell differentiation

Western blotting analysis demonstrated that tabersonine induced significant alterations in the expression levels of the differentiation-associated proteins C-Fos, C-Jun, and NFATc1 in osteoclast-like cells (Figure 5A). Semi-quantitative analysis of gray values revealed that the expression levels of C-Fos, C-Jun, and NFATc1 were markedly down-regulated in the tabersonine-treated groups (5 μM and 10 μM) relative to the control group (RANKL only) (p<0.01 or <0.001), suggesting a dose-dependent relationship (Figure 5B).

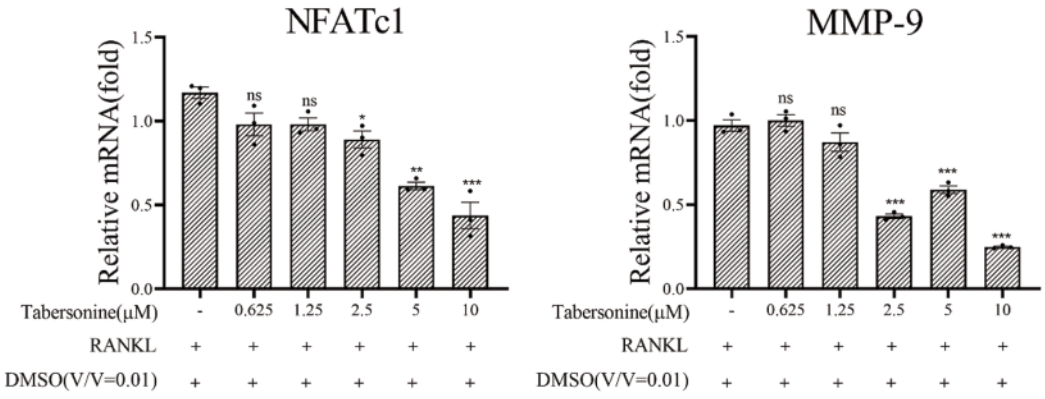


Figure 4. Tabersonine inhibits the expression of genes critical for osteoclast-like cell differentiation. RANKL induced RAW 264.7 cells for 3 d. Cellular RNA was extracted after 36 h of treatment with different concentrations of tabersonine. The cDNA was obtained by reverse transcription, and the key genes for osteoclast-like cell differentiation, MMP-9 and NFATc1 mRNA, were detected by qRT-PCR. Results are expressed as the means ± SEM. Ns, not statistical significance, *p<0.05, **p<0.01, ***p<0.001 *vs* control.

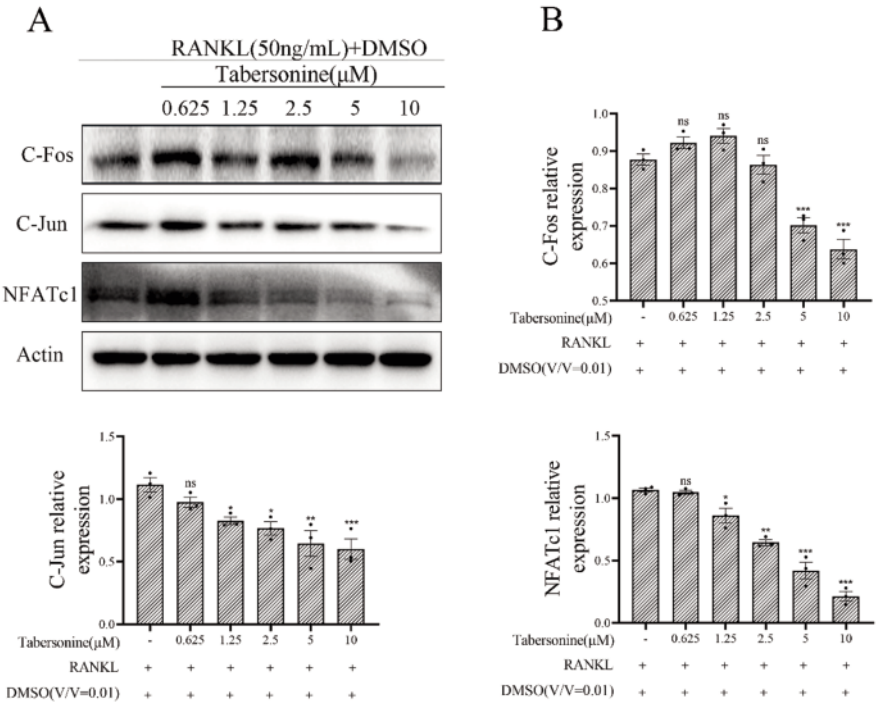


Figure 5. Tabersonine inhibits the expression of proteins associated with osteoclast-like cell differentiation. **A**) RANKL induced RAW 264.7 cells for 3 d; total cellular proteins were extracted after 36 h of treatment with different concentrations of tabersonine; the expression of NFATc1, C-Fos and C-Jun, key proteins for osteoclast-like cell differentiation, was detected by western blotting assay after protein concentration detection and quantification. **B**) Comparison of protein gray values for each group. Results are expressed as the means ± SEM. Ns, not statistical significance, *p<0.05, **p<0.01, ***p<0.001 *vs* control.

OPEN ACCESS

Morphologic effects of tabersonine on apoptosis of mature osteoclast-like cells

Experimental results indicated that nuclei in the control group (RANKL only) exhibited faint blue fluorescence of relatively uniform intensity, whereas nuclei in the Tabersonine-treated groups (0.625 μM, 1.25 μM, 2.5 μM, 5 μM, and 10 μM) displayed bright, heterogeneous blue fluorescence with elevated intensity (Figure 6).

Effect of tabersonine on ROS production in mature osteoclast-like cells

The results of the reactive oxygen species (ROS) experiments indicated a gradual rightward shift in the ROS peak with increasing concentrations of tabersonine (Figure 7A). ROS fluorescence levels exhibited a highly significant reduction in the 2.5 μM (59.27 ±0.58), 5 μM (64.57±0.75), and 10 μM (67.03±1.16) tabersonine groups compared with the control group (RANKL only)

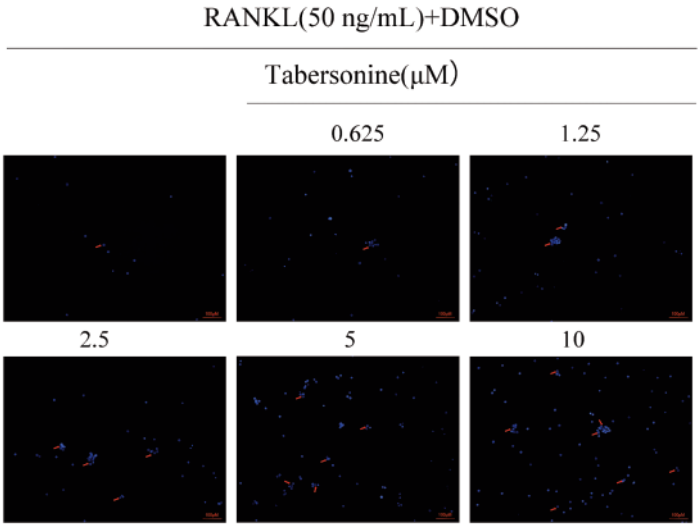


Figure 6. Tabersonine promotes apoptosis in mature osteoclast-like cells. RANKL induced RAW 264.7 cells for 3 d. After treatment with different concentrations of tabersonine for 36 h, the morphologic changes in the nuclei of mature osteoclast-like cells were observed by Hoechst 33258 staining (100×).

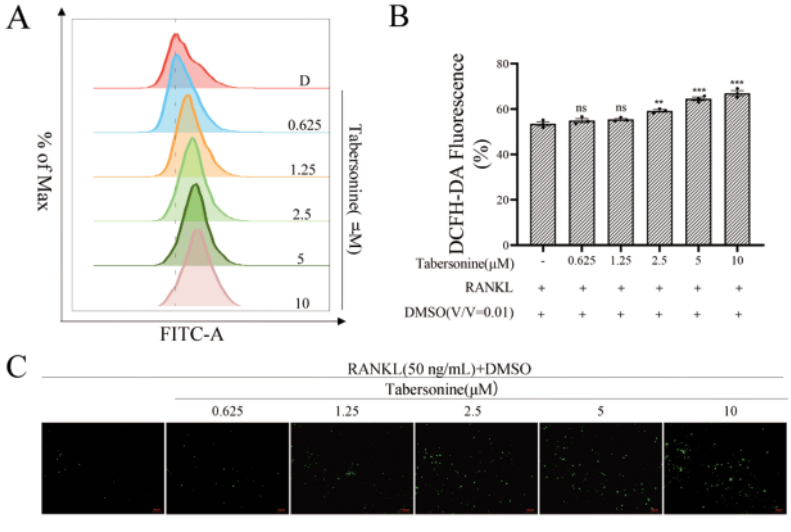


Figure 7.Tabersonine promotes ROS production in mature osteoclast-like cells. **A**) RANKL induced RAW 264.7 cells for 3 d; after treatment with different concentrations of tabersonine for 36 h, the cells were collected to determine the ROS content of each group by flow cytometry. **B**) Comparison of DCFH-DA fluorescence intensity between groups. Results are expressed as the means ± SEM; ns, not statistical significance, **p*<0.05, ***p*<0.01, ****p*<0.001 vs control. **C**) Representative fluorescence micrographs for qualitative ROS observation (100×).

(53.53±0.926) (p<0.01 or p<0.001), demonstrating a dose-dependent effect (Figure 7B). Furthermore, the probe was directly loaded onto ROS, and ROS generation was observed using a fluorescence microscope. The results revealed minimal green fluorescence in the control group (RANKL only), whereas pronounced DCF staining was evident in the 0.625 μM, 1.25 μM, 2.5 μM, 5 μM, and 10 μM Tabersonine groups (Figure 7C).

Effect of tabersonine on the expression levels of key genes for apoptosis in mature osteoclast-like cells

The findings indicated a significant increase in the mRNA levels of Caspase-3 and in the Bax/Bcl-2 mRNA ratio in osteoclast-like cells treated with 1.25 μM, 2.5 μM, 5 μM, and 10 μM Tabersonine, with highly significant differences observed (p<0.01 or p<0.001) in a dose-dependent manner relative to the control group (RANKL only) (Figure 8).

Effect of tabersonine on the levels of key proteins for apoptosis in mature osteoclast-like cells

The results of Western blotting demonstrated significant alterations in the expression levels of apoptosis-related proteins, including Caspase-3, Bax, Bcl-2, and Caspase-9, in the tabersonine-treated groups (Figure 9A). Semi-quantitative analysis of gray values indicated significant upregulation of the Caspase-3, Caspase-9, and Bax/Bcl-2 ratios in the 2.5 μM, 5 μM, and 10 μM Tabersonine groups relative to the control group (RANKL only), with highly significant differences observed (p<0.01 or p<0.001) in a dose-dependent manner (Figure 9B).

Effect of tabersonine on bone microstructure in osteoporotic mice

Micro-CT scan reconstruction revealed significant bone loss in the OVX group of mice (Figure 10A). This finding was supported by the data showing that Ct.Th (0.163±0.003), BMD (0.106±0.003), Tb.N (0.976±0.023), Tb.Th (0.048±0.000), and BV/TV (0.038±0.002) in the OVX group were markedly lower than those in the Sham group. Furthermore, Tb.Sp (0.37±0.004) was significantly higher in the OVX group compared with the Sham group, confirming substantial bone loss. In contrast, treatment with tabersonine resulted in significantly elevated levels of Ct.Th (0.175±0.002), BMD (0.132±0.003), Tb.N (1.377±0.003), Tb.Th (0.053±0.002), and BV/TV (0.056±0.002) relative to the OVX group. Additionally, Tb.Sp (0.339±0.004) was significantly lower in the tabersonine-treated mice, indicating that Tabersonine effectively mitigated bone loss (Figure 10B).

Effect of tabersonine on the structure of bone trabeculae in osteoporotic mice

Histological staining of H&E sections illustrated that the OVX group exhibited significant bone loss, characterized by sparse trabeculae in the cancellous bone region. In contrast, treatment with tabersonine led to a remarkable improvement in bone loss (Figure 11A). Additionally, statistical analysis of the TBA revealed a highly significant decrease (p<0.01) in the OVX group (9.08±0.311) compared with the Sham group (16.7±0.170), whereas the OVX + Tab group demonstrated a highly significant increase (p<0.01) in TBA (11.7±0.398) (Figure 11B).

Effect of tabersonine on the number of osteoclasts in osteoporotic mice

TRAP staining of femoral tissue sections revealed enlarged burgundy osteoclast-lined surfaces around trabecular bone in OVX mice. Conversely, tabersonine treatment markedly lowered the osteoclast surface fraction (Figure 12A). Quantitative analysis of osteoclast surface area around bone trabeculae revealed that Oc.S/BS was significantly elevated in the OVX group (1.03±0.056) compared with the Sham group (0.259±0.015) (p<0.001). In contrast, Oc.S/BS was significantly reduced in the Tabersonine-treated group (0.503±0.038) (p<0.001) (Figure 12B).

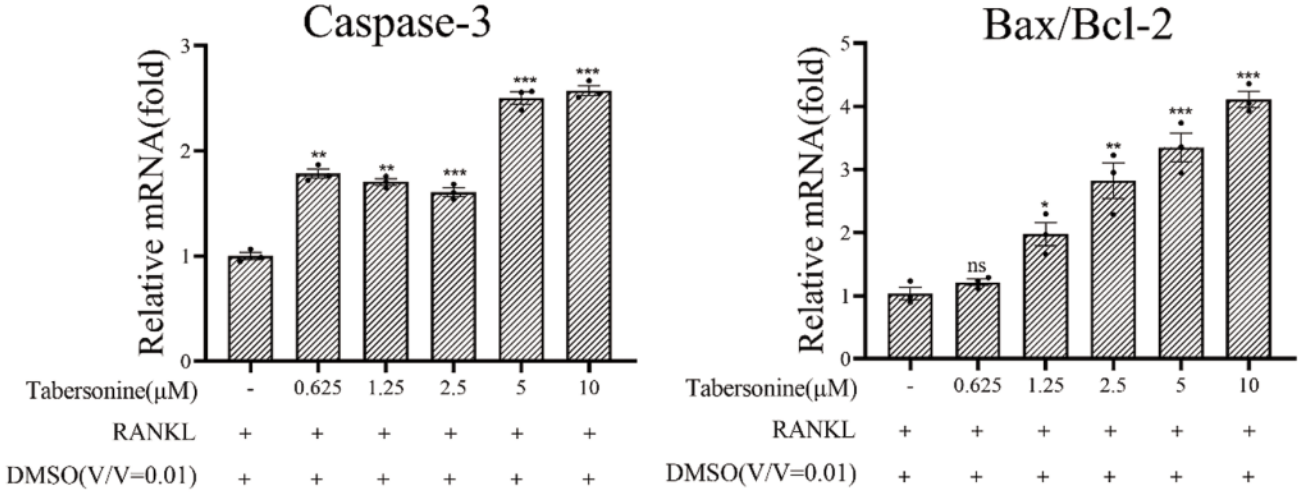


Figure 8. Tabersonine affects the expression levels of apoptosis-related genes in mature osteoclast-like cells. RANKL induced RAW264.7 cells for 3 d. After treatment with different concentrations of tabersonine for 36 h, the cells were collected for total RNA extraction. After reverse transcription to obtain cDNA, the expression of key genes of osteoclast-like cell apoptosis, Caspase-3, Bax and Bcl-2, was detected by qRT-PCR. Results are expressed as the means ± SEM. ns, not statistical significance, *p<0.05, **p<0.01, ***p<0.001 *vs* control.

OPEN ACCESS

Discussion

Tabersonine, a naturally occurring indole alkaloid isolated from the medicinal plant periwinkle, possesses a range of biological activities. Previous studies have demonstrated that tabersonine mitigates obese kidney injury by inhibiting NF-κB-mediated inflammation,[12] binds to transforming growth factor-activated kinase 1 (TAK1) to inhibit obesity-related cardiomyopathy,[14] and attenuates acute lung injury by inhibiting TRAF6 ubiquitination and the p38/MK2 signaling pathway.[18] However, to date, no reports have documented the effects of tabersonine on osteoclast activity or bone loss *in vivo*. This study found that tabersonine inhibited RANKL-induced differentiation of RAW264.7 cells into osteoclast-like cells and promoted apoptosis in mature osteoclast-like cells. Furthermore, animal experiments demonstrated that tabersonine could effectively improve bone loss in osteoporotic mice. Osteoclasts express TRAP, which serves as a reliable marker for identifying these cells. TRAP, along with other enzymes, plays a critical role in the degradation of the bone matrix by osteoclasts. TRAP staining is a specific method utilized for the identification of osteoclasts.[19] In the present study, TRAP staining results demonstrated that tabersonine inhibited the formation of osteoclast-like cells induced in vitro by differentiation. Furthermore, TRAP staining results from animal experiments indicated that tabersonine reduced the proportion of area occupied by osteoclasts in femoral tissues. Osteoclasts, which are derived from the hematopoietic stem cell lineage, represent the sole cell type in the organism with bone resorption activity.[20] The differentiation of osteoclasts is co-regulated by various cells and their associated products. Upon binding of RANKL and M-CSF to their respective receptors RANK and c-Fms on osteoclast precursor cells, a cascade of key transcription factors essential for osteoclast differentiation and activation is triggered.[21] NFATc1 is a pivotal nuclear transcription factor downstream of the RANKL/RANK signaling pathway that is involved in osteoclast differentiation. Previous studies have shown that NFATc1-deficient osteoclast precursor cells fail to differentiate into mature osteoclasts, whereas osteoclast precursor cells with high levels of NFATc1 expression can differentiate into osteoclasts even in the absence of RANKL.[22] Moreover, NFATc1 synergizes with PU.1, C-Fos, and MMP-9, with these genes collec-

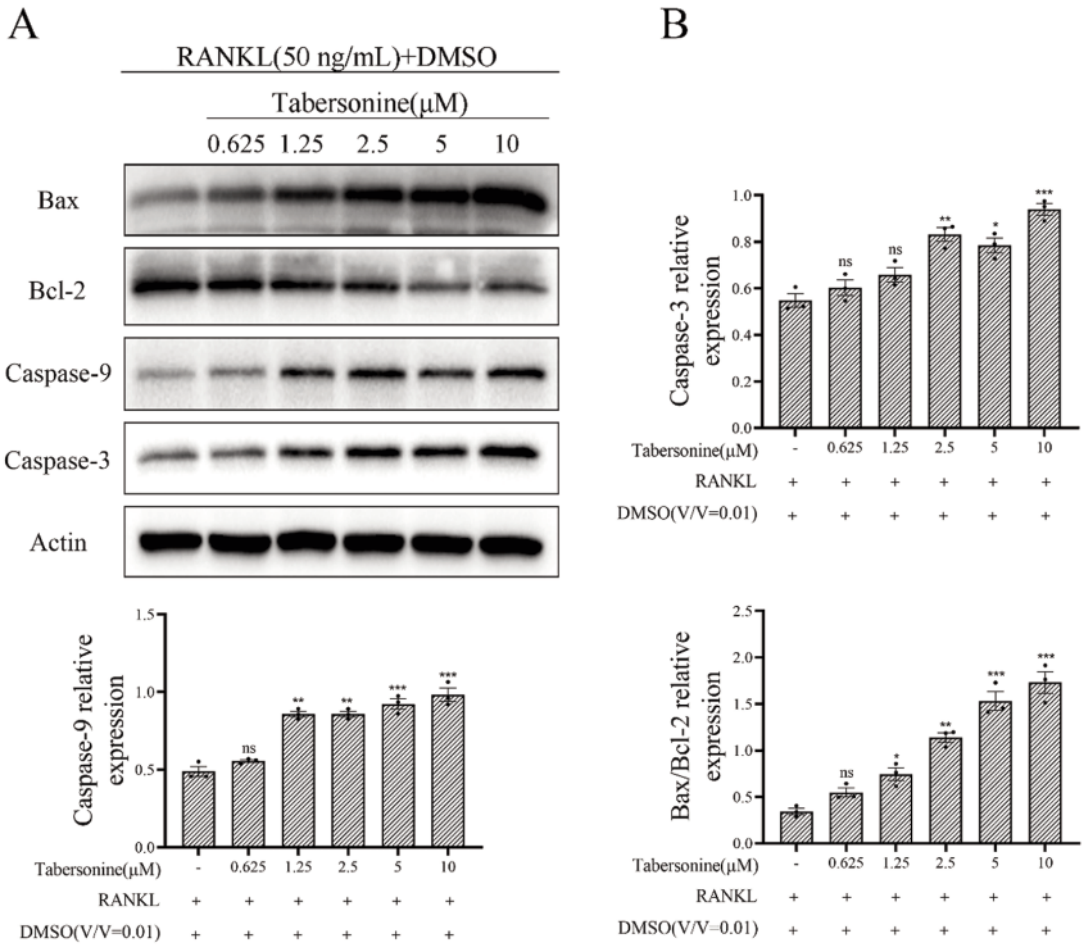


Figure 9. Effect of tabersonine on apoptosis-related proteins in mature osteoclast-like cells. **A**) RANKL induced RAW 264.7 cells for 3 d; after treatment with different concentrations of tabersonine for 36 h, the cells were collected to extract the total proteins, and the expression of the key proteins of osteoclast-like apoptosis, Caspase-3, Caspase-9, Bax, and Bcl-2, were detected by western blotting assay. **B**) Comparison of protein gray values for each group. Results are expressed as the means ± SEM. ns, not statistical significance, *p<0.05, **p<0.01, ***p<0.001 *vs* control.

tively regulating osteoclast formation and activity.[23] MMP-9 has been implicated in the process of osteoclast-mediated bone resorption, contributing to the degradation of organic components of the bone matrix.[24] C-Fos is a crucial factor for the activation of NFATc1, as the C-Fos gene combines with the C-Jun gene to form the activator protein-1 (AP-1) complex, which is essential for osteoclast development.[25] In our study, Tabersonine was found to inhibit the expression of MMP-9 and NFATc1 genes, as well as to suppress the expression of NFATc1, C-Fos, and C-Jun proteins. These results suggest that Tabersonine effectively inhibits the expression of specific genes and proteins associated with the differentiation and activation of osteoclast-like cells. Notably, the three transcription factors display differential sensitivity to tabersonine. C-Jun and its downstream target NFATc1 are markedly suppressed at concentrations as low as 1.25 μM, whereas C-Fos exhibits significant downregulation only at ≥5 μM. As an upstream AP-1 subunit, C-Jun is highly vulnerable to low-dose tabersonine, and NFATc1 follows suit as its direct target. At 0.625-2.5 μM, cellular compensatory pathways preserve basal C-Fos levels to counteract mild drug inhibition; robust suppression of C-Fos occurs only when the drug's inhibitory effect outweighs compensatory regulation at 5 μM and above. This graded sensitivity reveals the hierarchical osteoclastogenic signaling network and confirms that tabersonine inhibits osteoclast differentiation primarily via the C-Jun/NFATc1 axis.[26-28]

Microfilaments are essential components of the cytoskeleton found within the cytoplasm of cells, playing a crucial role in various physiological processes including the maintenance of cellular morphology, motility, division, and signal transduction. These microfilaments are primarily composed of actin, which exists in two intracellular forms: polymerized F-actin and free G-actin.[29] F-actin, which has a fibrillar structure, constitutes the primary form of microfilaments and is vital for the formation and activity of osteoclasts. Within osteoclasts, F-actin organizes into a characteristic gasket-like structure referred to as the actin ring or sealing zone. This structure delineates the microenvironment in which osteoclasts perform their bone resorption function, separating it from the surrounding extracellular space. Moreover, the F-actin sealing zone is proposed to serve as a functional indicator of osteoclast activation.[30] In the current study, tabersonine was observed to

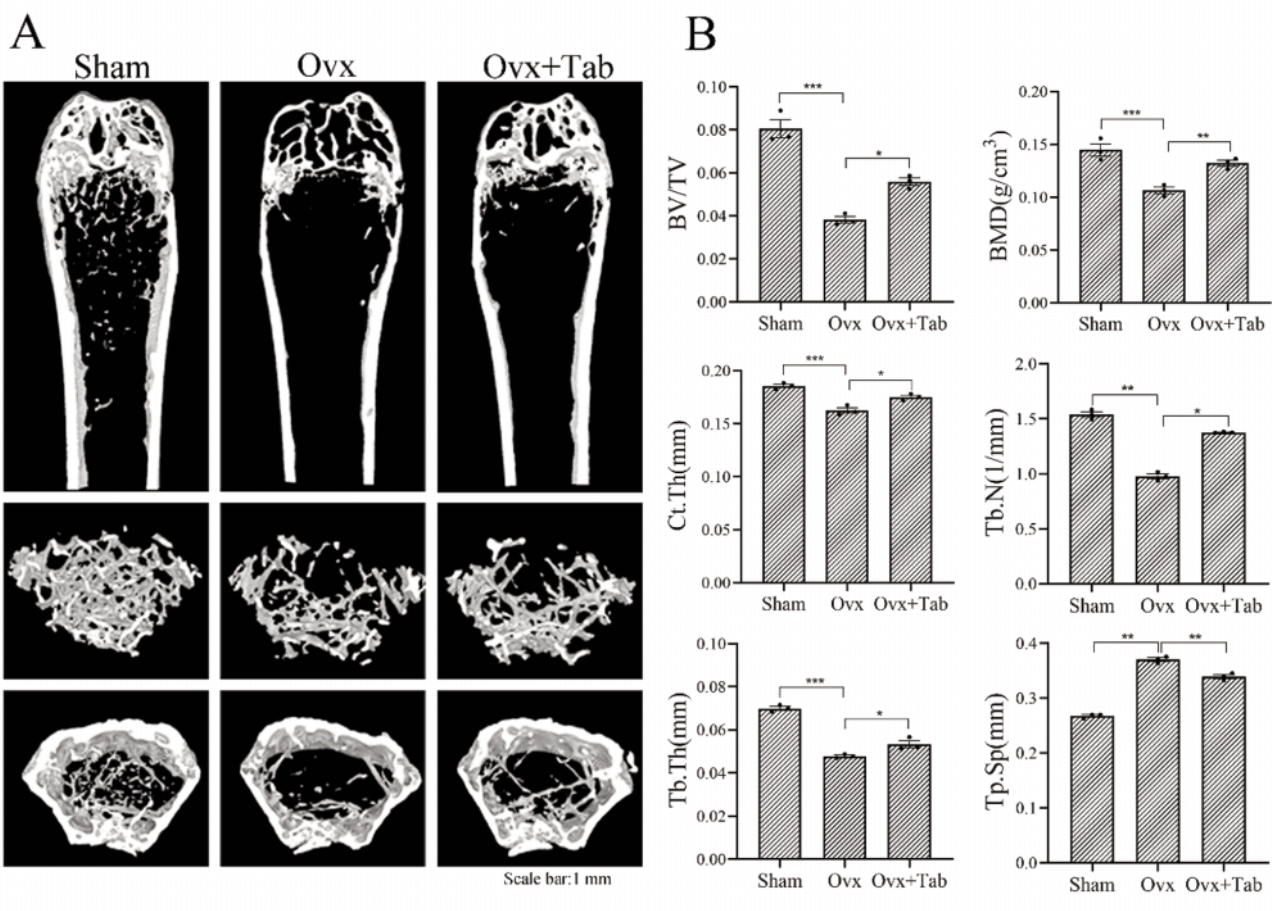


Figure 10. Tabersonine ameliorates bone loss in osteoporotic mice. **A**) Osteoporosis mouse model was established and Micro-CT scanning reconstruction was performed to analyze the bone loss status of mice in each group after tabersonine treatment. **B**) Bone volume / total volume (BV/TV), bone mineral density (BMD), cortical width (Ct.Th), trabecular number (Tb.N), trabecular thickness (Tb.N), trabecular thickness (Tb.Th) and trabecular separation (Tb.Sp) were compared. Results are expressed as the means ± SEM. ns, not statistical significance, *p<0.05, **p<0.01, ***p<0.001 *vs* control.

OPEN ACCESS

inhibit the formation of F-actin in osteoclast-like cells. Apoptosis, a form of programmed cell death, is integral to both pathological and physiological processes, including cellular homeostasis, tissue remodeling, and tumorigenesis.[31] Three primary pathways are recognized in classical apoptosis: the death receptor pathway, the mitochondrial apoptosis pathway, and the endoplasmic reticulum apoptosis pathway.[32] Research indicates that inducing apoptosis in osteoclasts is an effective strategy to counteract the reduction of bone mass caused by osteoclastic bone resorption.[33] Key indicators of apoptosis include morphological changes, alterations in mitochondrial membrane potential, DNA fragmentation, and variations in the expression levels of apoptosis-related proteins and genes. Hoechst 33258, a blue fluorescent dye with low cytotoxicity, penetrates cell membranes, serving as a straightforward and effective method for visualizing osteoclast apoptosis. In living cells, Hoechst 33258 staining binds to the minor groove of DNA within

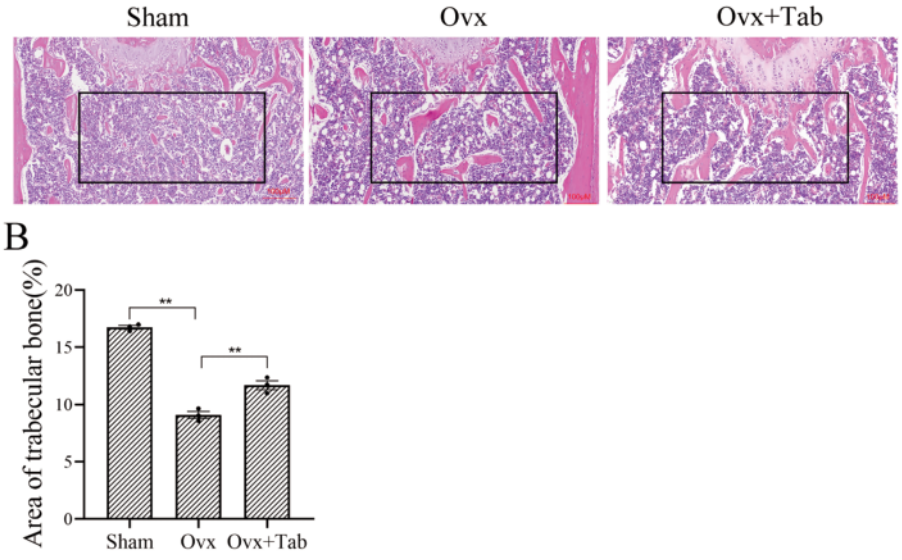


Figure 11. Tabersonine ameliorates bone loss in osteoporotic mice. **A**) Osteoporosis mouse model was established and H&E staining was performed to observe the condition of bone trabeculae in each group of mice after tabersonine treatment; scale bar: 100 μM. **B**) The ratio of the area of trabecular bone (ATB) to the area of trabecular bone was compared between the groups. Results are expressed as the means ± SEM. ns, not statistical significance, *p<0.05, **p<0.01, ***p<0.001 *vs* control.

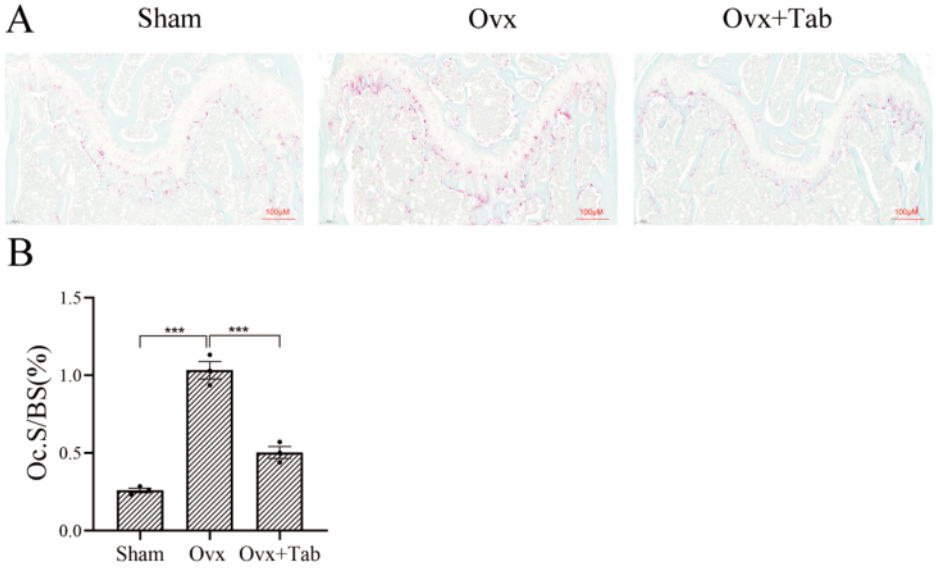


Figure 12. Tabersonine reduces the ratio of the osteoclasts surface to per unit bone surface (Oc.S/BS) in osteoporosis mice. **A**) Osteoporosis mouse model was established, and TRAP staining was performed to observe the distribution of osteoclasts around bone trabeculae in each group of mice after tabersonine treatment; scale bar: 100 μM. **B**) The ratio of the osteoclasts surface to per unit bone surface (Oc.S/BS) was comparatively analyzed for each group. Results are expressed as the means ± SEM. ns, not statistical significance, *p<0.05, **p<0.01, ***p<0.001 *vs* control.

AT-rich regions, such that normal nuclei appear rounded with pale blue fluorescence, whereas nuclei of apoptotic cells exhibit intense blue fluorescence due to DNA condensation resulting from DNase cleavage, often leading to fragmentation. In this study, osteoclast-like cells treated with tabersonine exhibited apoptotic characteristics, including nuclear condensation, dense staining, and elevated fluorescence intensity. These findings suggest that tabersonine promotes apoptosis in mature osteoclast-like cells.

ROS are one-electron reduction products of oxygen species in the body. It has been observed that when RANKL binds to its receptor on the cell surface, intracellular ROS production is stimulated, a crucial process that promotes the differentiation and formation of osteoclasts. However, elevated levels of ROS can lead to oxidative stress and subsequent cellular damage. Oxidative stress is frequently regarded as a significant contributor to aging and organ damage.[34] The underlying mechanism involves ROS, which can serve as a second messenger to upregulate pro-apoptotic protein expression in response to pro-apoptotic signaling, particularly when present at elevated levels. Additionally, ROS promotes changes in mitochondrial outer membrane permeability, activates the Caspase kinase family, and ultimately induces apoptosis.[35] This study found that tabersonine enhanced the generation of ROS in osteoclast-like cells, subsequently stimulating apoptosis in mature osteoclast-like cells.

The caspase family plays a pivotal regulatory role in apoptotic signaling,[36] particularly Caspase-3, which is known as the executor of apoptosis.[37] The Bcl-2 family (including Bax and Bcl-2) serves as a key regulator of mitochondrial apoptosis. The pro-apoptotic protein Bax penetrates the mitochondrial membrane, thereby initiating the caspase cascade reaction that leads to programmed cell death, whereas the apoptosis inhibitor Bcl-2 localizes to the outer mitochondrial membrane, where it obstructs the oligomerization of Bax and Bak. This action blocks the opening of voltage-dependent anion channels (VDACs) and inhibits apoptosis by limiting the release of cytochrome C.[38] This study found that Tabersonine enhanced the expression of Caspase-3 and Bax while simultaneously inhibiting the expression of Bcl-2.

Osteoporosis is a prevalent metabolic bone disease that can be classified into two categories: primary and secondary osteoporosis. Among the types of primary osteoporosis, postmenopausal osteoporosis is the most common, characterized primarily by a reduction in bone strength. Bone strength is assessed through two critical dimensions: bone density and bone mass. BMD serves as the primary determinant of bone strength and is considered the gold standard for diagnosing osteoporosis.[39] Additionally, bone microarchitecture plays a vital role in determining bone quality. The trabecular correlation index is an important metric reflecting changes in bone microstructure and serves as a key indicator for evaluating the onset and progression of osteoporosis.[40] Research indicates that in osteoporotic conditions, the deterioration of bone tissue microstructure is particularly pronounced in the trabecular and cortical bone. This deterioration is marked by a reduction in the number of trabecular structures, thinning of the cortical bone, and an increased susceptibility to damage. The clinical application of Micro-CT imaging to assess the skeletal structure of patients with osteoporosis and other bone disorders in three dimensions enhances our understanding of the associated pathological processes and treatment outcomes.[41] Micro-CT analyses revealed that mice in the OVX group exhibited significant bone loss; however, following tabersonine treatment, all osteoporosis-related indices improved markedly. Notable improvements included significant increases in BV/TV, Tb.N, Tb.Th, BMD, and Ct.Th, alongside a reduction in Tb.Sp. In addition, studies have demonstrated that estrogen inhibits both the differentiation and activity of osteoclasts. A decline in estrogen levels diminishes its inhibitory effect on osteoclast-mediated bone resorption, resulting in an increase in the number of osteoclasts and a decrease in apoptosis. This shift leads to an overall increase in bone loss.[42] The present study found that tabersonine significantly reduced the number of osteoclasts in the trabecular region of mouse bone, corroborating the findings from the *in vitro* experiments.

In conclusion, the combination of *in vitro* and *in vivo* studies demonstrated that tabersonine effectively inhibits the differentiation of osteoclast-like cells, promotes the apoptosis of mature osteoclast-like cells, and mitigates bone loss in osteoporotic mice.

References

1. Ensrud KE, Crandall CJ. Osteoporosis. Ann Intern Med 2024;177:ITC1-ITC16.
2. Walker MD, Shane E. Postmenopausal osteoporosis. N Engl J Med 2023;389:1979-91.
3. Foessl I, Dimai HP, Obermayer-Pietsch B. Long-term and sequential treatment for osteoporosis. Nat Rev Endocrinol 2023;19:520-33.
4. Stegen S, Carmeliet G. Metabolic regulation of skeletal cell fate and function. Nat Rev Endocrinol 2024;20:399-413.
5. Takegahara N, Kim H, Choi Y. Unraveling the intricacies of osteoclast differentiation and maturation: insight into novel therapeutic strategies for bone-destructive diseases. Exp Mol Med 2024;56:264-72.
6. Stegen S, Moermans K, Stockmans I, Thienpont B, Carmeliet G. The serine synthesis pathway drives osteoclast differentiation through epigenetic regulation of NFATc1 expression. Nat Metab 2024;6:141-52.
7. Dong Y, Kang H, Peng R, Liu Z, Liao F, Hu SA, et al. A clinical-stage Nrf2 activator suppresses osteoclast differentiation via the iron-ornithine axis. Cell Metab 2024;36:1679-95.e6.
8. Li Z, Li D, Chen R, Gao S, Xu Z, Li N. Cell death regulation: A new way for natural products to treat osteoporosis. Pharmacol Res 2023;187:106635.
9. Chen S, Jin J, Xu Z, Han H, Wu L, Li Z. Catalpol attenuates osteoporosis in ovariectomized rats through promoting osteoclast apoptosis via the Sirt6-ERα-FasL axis. Phytomedicine 2024;123:155262.
10. Reid IR. A broader strategy for osteoporosis interventions. Nat Rev Endocrinol 2020;16:333-9.
11. Etit D, Ögmundarson Ó, Zhang J, Krogh Jensen M, Sukumara S. Early-stage economic and environmental impact assessment for optimized bioprocess development: Monoterpenoid indole alkaloids. Bioresour Technol 2024;391:130005.
12. Qian C, Wang J, Lin W, Chen Y, Yang J, Liu M, et al. Tabersonine attenuates obesity-induced renal injury via inhibiting NF-κB-mediated inflammation. Phytother Res 2023;37:2353-63.
13. Xu HW, Li WF, Hong SS, Shao JJ, Chen JH, Chattipakorn N, et al. Tabersonine, a natural NLRP3 inhibitor, suppresses inflammasome activation in macrophages and attenuate NLRP3-driven diseases in mice. Acta Pharmacol Sin 2023;44:1252-61.
14. Chen Y, Lin W, Chen P, Ye B, Luo W, Wang X, et al. Tabersonine alleviates obesity-induced cardiomyopathy by binding to Transforming growth factor activated kinase 1 (TAK1) and inhibiting TAK1-mediated inflammation. Phytother Res 2023;37:860-71.
15. Sun X, Gan L, Li N, Sun S, Li N. Tabersonine ameliorates

OPEN ACCESS

osteoblast apoptosis in rats with dexamethasone-induced osteoporosis by regulating the Nrf2/ROS/Bax signalling pathway. AMB Express 2020;10:165.
16. Komori T. Animal models for osteoporosis. Eur J Pharmacol 2015;759:287-94.
17. Mu CR. Preparation and optimization of paraffin sections. New Discovery 2025;4:33-6.
18. Zhang D, Li X, Hu Y, Jiang H, Wu Y, Ding Y, et al. Tabersonine attenuates lipopolysaccharide-induced acute lung injury via suppressing TRAF6 ubiquitination. Biochem Pharmacol 2018;154:183-92.
19. Hayman AR. Tartrate-resistant acid phosphatase (TRAP) and the osteoclast/immune cell dichotomy. Autoimmunity 2008;41:218-23.
20. Veis DJ, O'Brien CA. Osteoclasts, master sculptors of bone. Annu Rev Pathol 2023;18:257-81.
21. Jung SY, Min BM. A vitronectin-derived dimeric peptide suppresses osteoclastogenesis by binding to c-Fms and inhibiting M-CSF signaling. Exp Cell Res 2022;418:113252.
22. Son A, Kang N, Oh SY, Kim KW, Muallem S, Yang YM, et al. Homer2 and Homer3 modulate RANKL-induced NFATc1 signaling in osteoclastogenesis and bone metabolism. J Endocrinol 2019;242:241-9.
23. Mun SH, Park PSU, Park-Min KH. The M-CSF receptor in osteoclasts and beyond. Exp Mol Med 2020;521239-54.
24. Al Mamun MA, Asim MMH, Sahin MAZ, Al-Bari MAA. Flavonoids compounds from Tridax procumbens inhibit osteoclast differentiation by down-regulating c-Fos activation. J Cell Mol Med 2020;24:2542-51.
25. Jiang T, Xia T, Qiao F, Wang N, Jiang Y, Xin H. Role and regulation of transcription factors in osteoclastogenesis. Int J Mol Sci 2023;24:16175.
26. Yang Q, Guo J, Zheng J, Chen Y, Zou B, Li R, et al. Polyphyllin VII protects from breast cancer-induced osteolysis by suppressing osteoclastogenesis via c-Fos/NFATc1 signaling. Int Immunopharmacol 2023;120:110316.
27. Zhang L, Yang Y, Liao Z, Liu Q, Lei X, Li M, et al. Genetic and pharmacological activation of Hedgehog signaling inhibits osteoclastogenesis and attenuates titanium particle-induced osteolysis partly through suppressing the JNK/c-Fos-NFATc1 cascade. Theranostics 2020;10:6638-60.
28. Nakagawa S, Omori K, Nakayama M, Mandai H, Yamamoto S, Kobayashi H, et al. The fungal metabolite (+)-terrein abrogates osteoclast differentiation via suppression of the RANKL signaling pathway through NFATc1. Int Immunopharmacol 2020;83:106429.
29. Dominguez R, Holmes KC. Actin structure and function. Annu Rev Biophys. 2011;40:169-86.
30. Lee BS. Myosins in osteoclast formation and function. Biomolecules 2018;8:157.
31. Yuan L, Zhao N, Wang J, Liu Y, Meng L, Guo S, et al. Major vault protein (MVP) negatively regulates osteoclastogenesis via calcineurin-NFATc1 pathway inhibition. Theranostics 2021;11:7247-61.
32. Teitelbaum SL. The osteoclast and its unique cytoskeleton. Ann NY Acad Sci 2011;1240:14-7.
33. Roux S, Lambert-Comeau P, Saint-Pierre C, Lépine M, Sawan B, Parent JL. Death receptors, Fas and TRAIL receptors, are involved in human osteoclast apoptosis. Biochem Biophys Res Commun 2005;333:42-50.
34. Tai TW, Chen CY, Su FC, Tu YK, Tsai TT, Lin CF, et al. Reactive oxygen species are required for zoledronic acid-induced apoptosis in osteoclast precursors and mature osteoclast-like cells. Sci Rep 2017;7:44245.
35. Wong SW, Huang BW, Hu X, Ho Kim E, Kolb JP, Padilla RJ, et al. Global deletion of Optineurin results in altered type I IFN signaling and abnormal bone remodeling in a model of Paget's disease. Cell Death Differ 2020;27:71-84.
36. Van Opdenbosch N, Lamkanfi M. Caspases in cell death, inflammation, and disease. Immunity 2019;50:1352-64.
37. Eskandari E, Eaves CJ. Paradoxical roles of caspase-3 in regulating cell survival, proliferation, and tumorigenesis. J Cell Biol 2022;221:e202201159.
38. Birkinshaw RW, Czabotar PE. The BCL-2 family of proteins and mitochondrial outer membrane permeabilisation. Semin Cell Dev Biol 2017;72:152-62.
39. Roux C, Briot K. Current role for bone absorptiometry. Joint Bone Spine 2017;84:35-7.
40. Xiong Y, Huang CW, Shi C, Peng L, Cheng YT, Hong W, et al. Quercetin suppresses ovariectomy-induced osteoporosis in rat mandibles by regulating autophagy and the NLRP3 pathway. Exp Biol Med (Maywood) 2023;248:2363-80.
41. Chatterjee M, Faot F, Correa C, Kerckhofs J, Vandamme K. Is the jaw bone micro-structure altered in response to osteoporosis and bisphosphonate treatment? A micro-CT analysis. Int J Mol Sci 2021;22:6559.
42. Ryoo GH, Moon YJ, Choi S, Bae EJ, Ryu JH, Park BH. Tussilagone promotes osteoclast apoptosis and prevents estrogen deficiency-induced osteoporosis in mice. Biochem Biophys Res Commun 2020;531:508-14.

Received: 8 February 2026. Accepted: 8 October 2026.

This work is licensed under a Creative Commons Attribution-NonCommercial 4.0 International License (CC BY-NC 4.0).
©Copyright: the Author(s), 2026
Licensee PAGEPress, Italy
European Journal of Histochemistry 2026; 70:4546
doi:10.4081/ejh.2026.4546

Publisher's note: all claims expressed in this article are solely those of the authors and do not necessarily represent those of their affiliated organizations, or those of the publisher, the editors and the reviewers. Any product that may be evaluated in this article or claim that may be made by its manufacturer is not guaranteed or endorsed by the publisher.